JOURNAL OF THERMOPHYSICS AND HEAT TRANSFER
Vol. 19, No. 1, January–March 2005

Impingement Heat Transfer, Part II: Effect of Streamwise Pressure Gradient

Ryan Hebert,* Srinath V. Ekkad,† and Lujia Gao*
Louisiana State University, Baton Rouge, Louisiana 70803
and
Ronald S. Bunker‡
General Electric Global R&D Center, Niskayuna, New York 12309

This is Part II of a two-part paper on jet-impingement heat transfer. The effect of streamwise pressure gradient on jet-impingement heat transfer is investigated. In realistic configurations, impingement arrays do not always impinge in channels that have parallel walls. Converging channels create positive pressure gradient, and diverging channels create adverse pressure gradient. In this study, the effect of nonparallel walls on jet-impingement heat transfer is investigated. Firstly for impingement arrays with jet-to-jet streamwise and spanwise spacing of four-hole diameters and eight-hole diameters and then for the linearly stretched arrays discussed in Part I. Two jet Reynolds numbers are studied for all cases for $Re = 6 \times 10^3$, and 10^3. Also, the jet height-to-diameter ratio is increased from 1 to 5 to generate the adverse pressure gradient and decreased from 5 to 1 to generate the positive pressure gradient. Results show that the effect of streamwise pressure gradient alters the flow distribution causing significant variations in heat-transfer distributions. Accelerating flow causes streamwise jet stretching, whereas decelerating flow causes spanwise jet stretching. The results for converging and diverging channels are compared with results for parallel plate channels with different spacing to compare the effect of the streamwise pressure gradient.

Nomenclature

A	=	constant in Florschuetz et al. correlation[5]
B	=	constant in Florschuetz et al. correlation[5]
D	=	impingement jet hole diameter (0.635 cm)
G	=	mass flux, Kg/m$^2 \cdot$ s
h	=	local convection heat-transfer coefficient, W/m$^2 \cdot$ K
k	=	thermal conductivity of Plexiglas® surface, W/m $\cdot$ K
k_{air}	=	thermal conductivity of air, W/m $\cdot$ K
Nu	=	Nusselt number, hD/k_{air}
Pr	=	Prandtl number, ν/α
Re	=	Reynolds number, $\rho V_j D/\mu$
T_i	=	initial temperature of test section, K
T_m	=	mainstream temperature of the flow, K
T_w	=	color-change temperature of the liquid crystal (red-to-green), K
t	=	time of liquid crystal color change, s
UD	=	uniform diameter array
V_j	=	average jet velocity, m/s
VD	=	variable diameter array
X	=	streamwise distance of the impingement surface (exit flow direction), m
Y	=	spanwise distance on the impingement surface, m
Z	=	jet hole-to-target wall spacing, also H, m
α	=	thermal diffusivity of Plexiglas, m^2/s
μ	=	fluid dynamic viscosity, kg/(m $\cdot$ s)
ν	=	kinematic viscosity, m^2/s
τ	=	time step
ϕ	=	crossflow coefficient from Kercher and Tabakoff

Subscripts

c	=	crossflow
j	=	jet

Introduction

IMPINGEMENT-JET arrays are widely used as a heat-transfer enhancement method for cooling or heating purposes. This scheme is used extensively in gas turbine systems because of the high heat-transfer capabilities of the jet. Typically, the jets are in arrays, and the arrangement of the arrays is determined based on cooling requirements on the airfoil or shroud surfaces. The arrays are not always in the square form where the jet-to-jet spacing is evenly distributed along the surface. Also, the jet-to-impingement surface distance varies at different locations. This is typically a regular array of holes that can appear stretched in the streamwise and spanwise direction resulting in increased spacing for the downstream holes. Their use is essentially to increase surface cooling coverage, where arrays are tailored or varied according to the external heat loading. This method is not only used to produce distributed cooling on hot surfaces with limited coolant usage but also to counteract the effects of crossflow degradation. This degradation can be especially severe for stretched arrays. These linear stretched arrays are an important an issue for the backside cooling of dry low emulsion (DLE) combustor liners.

Previous studies on jet-impingement heat transfer[1–7] summarized findings relating to parametric effects of jet geometry, temperature, crossflow, turbulence, etc. on impingement heat and mass transfer. Kercher and Tabakoff[2] and Florschuetz et al.[5] determined that the heat-transfer characteristics for jet array impingement are affected by the crossflow. They presented correlations for both inline and staggered hole patterns including effects of crossflow on impingement heat transfer. A comprehensive literature survey of all of the jet-impingement studies and the correlations are summarized by Downs and James.[8] Huber and Viskanta[9,10] studied the effect of jet-to-jet spacing and also compared heat transfer for perimeter and center jets in a confined, impinging array of axisymmetric air jets. All of the preceding studies presented the effects of various parameters on jet-impingement heat transfer. Van Treuren et al.[11] were the first to present detailed distributions under impinging jets.

Received 25 February 2004; revision received 28 June 2004; accepted for publication 28 June 2004.

*Graduate Research Assistant, Mechanical Engineering Department.
†Associate Professor, Mechanical Engineering Department. Member AIAA.
‡Senior Scientist. Member AIAA.

They measured both local heat-transfer coefficient and adiabatic wall temperature under the impinging jets. Huang et al.[12] studied the effect of crossflow direction on impingement heat transfer for a square array of jet holes. They investigated only one jet-to-wall distance. They indicated that crossflow effect is minimal when the flow exits in both directions after impingement. Recently, Bailey and Bunker[13] studied the effect of jet array geometry by varying the spacing in a square array that looked at arrays of spacing ($X/D \times Y/D$) 3×3, 6×6, and 9×9. They also varied the jet plate-to-target wall distance ratio (Z/D) from 1.25 to 5.5. They presented a modified Florschuetz et al.[5] correlation to accommodate their new. Ekkad et al.[14] presented heat-transfer distributions for inline square arrays of spacing 4×4, 8×8, and rectangular arrays of spacing of four in the streamwise direction and eight in the spanwise direction. They also varied their jet-to-wall spacing H/D from 1 to 5. They clearly showed that closer spacing increases the jet-to-jet interaction and produces higher heat transfer in the regions between jets. The first part of the paper, Gao et al.,[15] studied the effect of linearly stretched arrays on impingement heat transfer. Linearly stretched arrays have increasing streamwise and spanwise spacing between holes in the downstream direction. Two different arrays, one with uniform diameter holes and another with increasing diameter holes, were studied. Results showed that the increasing diameter arrays produced higher heat-transfer coefficients than the uniform diameter array. Also, the correlations[2,3] underpredicted the heat-transfer coefficients as a result of overprediction of crossflow effects. Both Ekkad et al.[14] and Gao et al.[15] studied the effect of jet-to-wall spacing for three Z/D values of 1, 3, and 5.

In this study, the effect of streamwise pressure gradient is considered for the array geometries studied by Ekkad et al.[14] and Gao et al.[15] In real geometries, there is possibility of impingement occurring on plates that are not parallel to each other, resulting in the streamwise pressure gradient. This can be positive or adverse. The goal is to compare the results for each array geometry with even spacing to varying spacing channels to compare the effect of streamwise pressure gradient. This is the first study to focus on this aspect of jet-impingement cooling. The effect of jet average Reynolds number is also investigated. The converging and diverging channel data will be compared with the different jet-to-wall spacing results from Refs. 14 and 15.

Test Apparatus and Description

The test apparatus and section are described in detail in the Part I paper. The material will not be repeated in this paper. The base regular array jet plate has a square matrix of 11×11 holes of diameter 0.635 cm spaced four hole diameters apart in both directions (streamwise and spanwise). To vary the jet array configuration, some holes are taped, and some holes are left open to create different arrays for this study. Figure 1a shows the jet plate with all holes open. All configurations on this plate are arranged to obtain an array of 25 impingement holes with five holes in the spanwise direction and five holes in the streamwise direction. Figure 1b shows the first configurations where the holes are spaced four-hole diameters apart in both directions and is called the 4×4 array. Figure 1c shows the next regular configuration where the holes are spaced eight hole diameters apart in both directions and is called the 8×8 array. The linearly stretched arrays are the same used in Part I and will not be described. Both the plated with uniform diameter holes and variable diameter holes are used for the pressure gradient studies.

The spacing between the jet plate and impingement plate Z/D can be varied by changing the wall spacers along the three closed sides of the impingement channel. Spacers in the shape of right triangles are used to produce configurations with Z/D values that change in the flow direction from $Z/D = 5$ to 1, which in turn varies the cross-sectional area. The configuration with $Z/D = 5$ at the exit and a positive cross-sectional area change is called the diverging case. The converging case has a negative area change with $Z/D = 1$ at the exit. Figure 2a shows the diverging plate configuration with the flow direction to the right, and Fig. 2b shows the converging case.

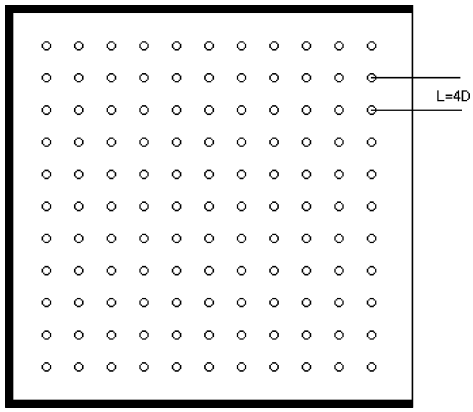

a) Original jet plate

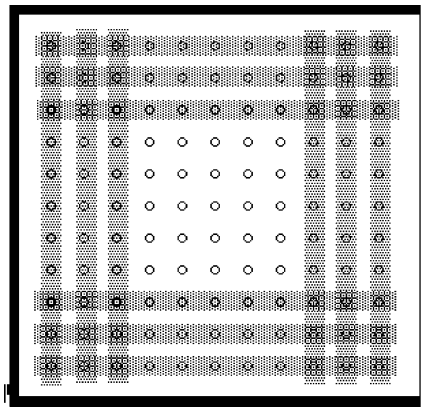

b) Jet plate with spacing 4

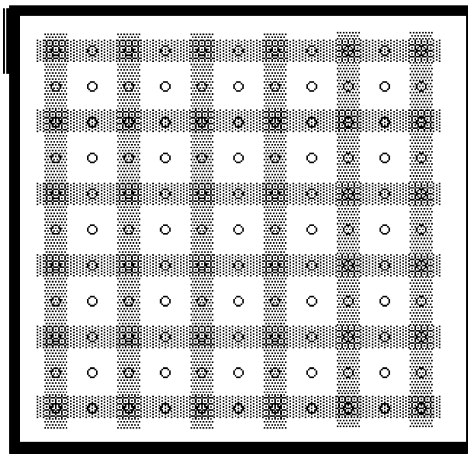

c) Jet plate with spacing 8

Fig. 1 Regular-impingement arrays.

Procedure and Analysis

The procedure and data reduction are identical as Part I and are not repeated for sake of redundancy. Uncertainly analysis also remains identical.

Results and Discussions

Regular Arrays

Jet average Reynolds numbers of 6×10^3 and 10^3, based on hole diameter, were examined in this study. The exit flow direction is from bottom to top, and the impingement is out of the page. Although detailed two-dimensional field measurements were obtained for the entire heat-transfer surface, the results are not presented. The spanwise-averaged results were obtained from the detailed two-dimensional maps.

Figures 3 and 4 compare the effect of even Z/D spacing and variable Z/D spacing on spanwise averaged Nusselt number for

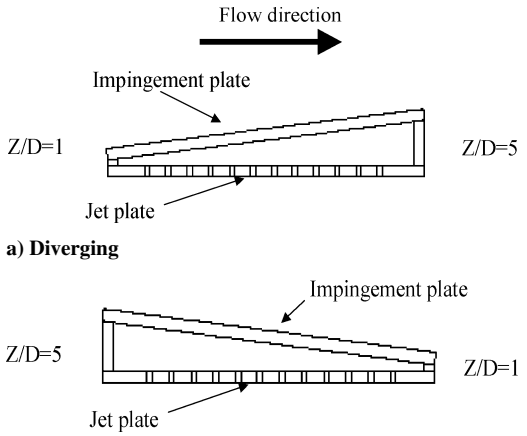

Fig. 2 Jet and impingement plate configurations.

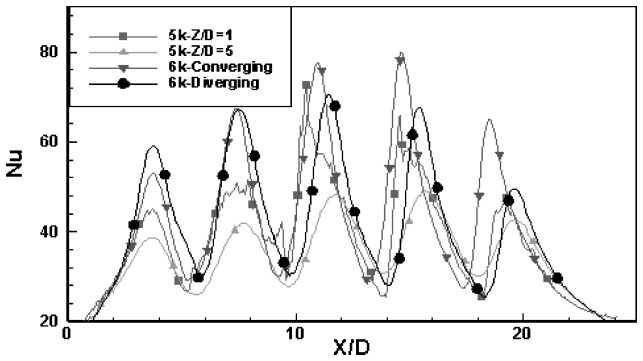

Fig. 3 Spanwise-averaged Nusselt numbers for 4 × 4 at $Re_D = 5 \times 10^3$ and 6×10^3.

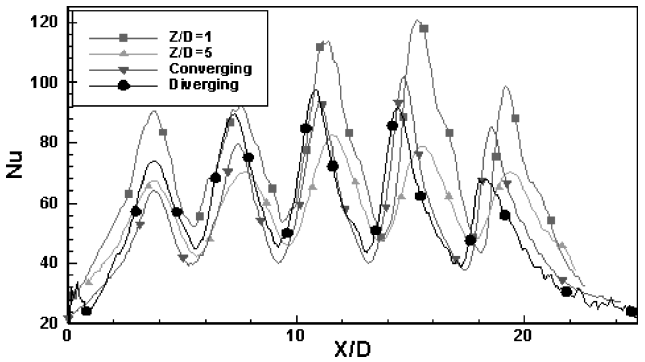

Fig. 4 Spanwise-averaged Nusselt numbers for 4 × 4 at $Re_D = 10^3$.

the 4×4 configuration at different Reynolds numbers. The Nusselt numbers are plotted against normalized flow direction X/D. The X/D reference location is just upstream of the first row of holes in that array. The overall X/D for the 4×4 case was 25 and the first jet is located at about 3.75. Figure 3 presents the spanwise-averaged Nusselt numbers for a 4×4 case with Z/D spacing of 1 and 5 at $Re_D = 5 \times 10^3$, published by Ekkad et al.[14] It also displays data for converging and diverging channels for the 4×4 case at $Re_D = 6 \times 10^3$. The $Z/D = 1$ and 5 configurations correlate to the entrance and exit of the converging and diverging cases. At $Re_D = 6 \times 10^3$, the Nusselt number values are lowest at the first jet, about 50. This correlates to the largest Z/D spacing. The maximum Nusselt number occurs at the fourth jet with an approximate value of 80. Again, this is seen because the fourth jet is located at a smaller Z/D spacing. Despite the clear Z/D relationship, the maximum Nusselt number does not occur at the lowest Z/D spacing. The reason that the fourth jet sees the maximum heat transfer is that at the

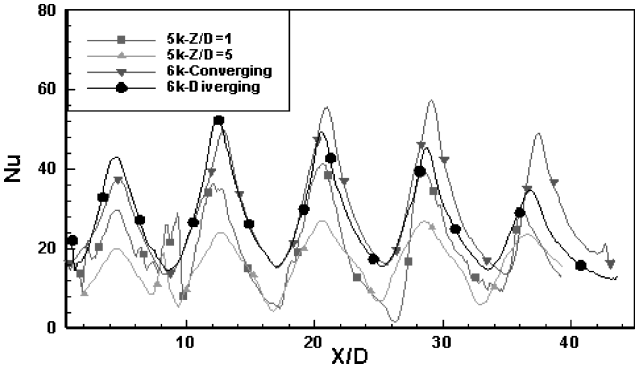

Fig. 5 Spanwise-averaged Nusselt numbers for 8x8 at $Re_D = 5 \times 10^3$ and 6×10^3.

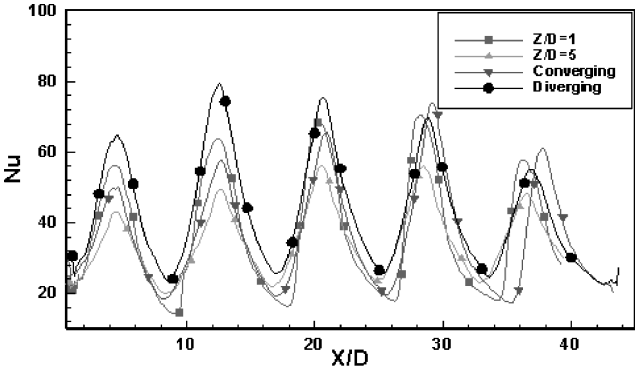

Fig. 6 Spanwise-averaged Nusselt numbers for 4 × 4 at $Re_D = 10^3$.

location of minimum plate spacing, the fifth jet, the crossflow from the previous four holes begins to have a significant effect on the jet flow and decreases impingement cooling. Conversely, the first two jets of the diverging case are shown to have higher Nusselt numbers than the latter two jets of the array.

Figure 4 shows the spanwise averaged Nusselt numbers for $Z/D = 1$, $Z/D = 5$, converging, and diverging for $Re_D = 10^3$. The heat transfer under and between the jets is significantly higher for this case compared to $Re_D = 6 \times 10^3$. The increase in cooling between the jets is a result of a stronger mixing effect. The same relationship between increased heat transfer on the smaller Z/D side of the converging case (flow exit) and the smaller Z/D spacing of the diverging case can still be seen. Finally, the crossflow again decreases the heat transfer on the last jet of the converging case and causes the maximum Nusselt number to occur at the fourth jet.

These same effects of Z/D spacing on spanwise-averaged Nusselt number can be seen in Figs. 5 and 6 for the 8×8 configuration at $Re_D = 6 \times 10^3$ and 10^3. Note in Fig. 5 the difference in Nusselt number values of the converging and diverging case at the first and last jets is quite similar to the difference between the $Z/D = 1$ and 5 cases. This is less evident in Fig. 5 because there tests run at $Re_D = 5 \times 10^3$ for $Z/D = 1$ and 5 and are compared to tests run at $Re_D = 6 \times 10^3$ for the converging and diverging cases. For the 8×8 cases, the highest Nusselt number under a jet is only 80 and 55 for $Re_D = 10^3$ and 6×10^3, respectively, compared to 120 and 80 for the 4×4 configurations. It clearly shows that increased jet spacing not only reduced the heat transfer in the region between the jets but also underneath the jets because of less jet interaction. Finally, also note that even though the Z/D spacing increases with each consecutive row of impingement jets for the diverging configuration the difference in heat transfer between the fourth and fifth jet for all cases is equivalent to the drop off in heat transfer as a result of crossflow for the converging case. This shows that crossflow causes little reduction in Nusselt numbers in the diverging study.

Linearly Stretched Arrays

For all cases in this study, the jet Reynolds numbers and local Nusselt numbers are based on average hole diameter and average

jet velocity. For all of the regular arrays and the uniform diameter plate, the uniform diameter and the average diameter are the same at 0.635 cm. For the variable diameter, the average diameter is 0.4318 cm.

Flow measurements were performed by Gao et al.[15] to estimate the amount of mass flow through each row of holes and the amount of crossflow effect for parallel plate impingement. The percent mass flow compared to the total mass flow through each hole and the amount of crossflow at the hole location are presented for stretched arrays in Part I. This flow information is critical towards predicting heat-transfer coefficients from correlations presented by Kercher and Tabakoff[2] and Florschuetz et al.[5] Again, these flow distributions were determined for parallel jet and impingement plate configuration. For this situation the flow characteristics were found to be independent of Z/D spacing, given it was constant, because the pressure differences between first row to exit of the impingement channel show minimum variations with changes in Z/D. To more accurately determine the amount of crossflow found in converging and diverging channels, the significant pressure gradients produced by variable Z/D spacing would have to be accounted for in this calculation.

Spanwise-Averaged Distributions

Figures 7 and 8 present the effect of Z/D spacing on spanwise-averaged Nusselt number at different Reynolds numbers for the uniform diameter configuration. The Nusselt numbers are plotted against normalized flow direction X/D. The location of the first impingement jet is $X/D=2$ and the overall $X/D=44$. Figure 7 presents the spanwise-averaged Nusselt numbers for $Z/D=1$, $Z/D=5$ (Ref. 15), converging and diverging at $Re_D=6\times10^3$. The highest heat transfer is realized at the first rows of jets for the diverging case because at this location both the Z/D spacing and the crossflow effects are at a minimum. The Nusselt-number average is around 65–75 for these first two rows in the diverging channel. Also, notice the extreme correlation between the spanwise-averaged Nusselt-number values for the first few rows of the both converging and diverging to $Z/D=5$ and 1, respectively. This relationship is also seen at the flow exit with $Z/D=1$ for converging and $Z/D=5$ for diverging; however, the similarity is not as prevalent as the first jet rows because at the downstream locations crossflow begins to have significant effect on heat transfer, especially for the converging case. These Z/D spacing similarities are also seen in the $Re_D=10^3$ case seen in Fig. 8. However, the increased Reynolds number causes much more crossflow interaction, and the correlation of converging and diverging to constant Z/D spacing is not as evident.

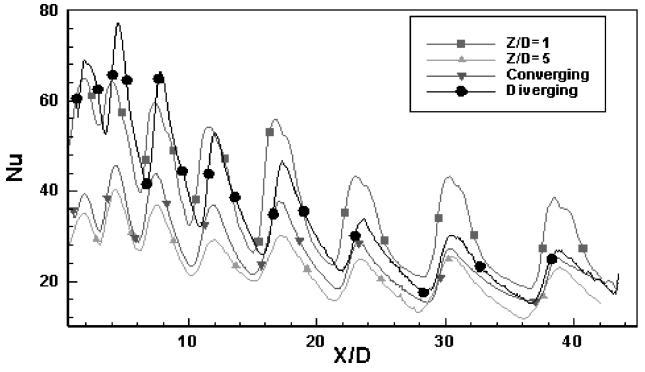

Fig. 7 Spanwise-averaged Nusselt numbers for uniform diameter configuration at $Re_D=6\times10^3$.

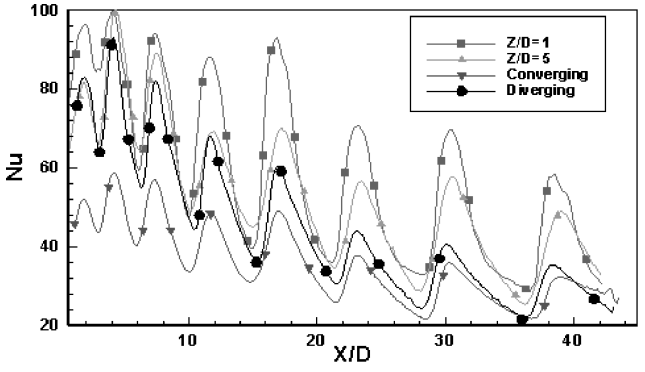

Fig. 8 Spanwise-averaged Nusselt numbers for uniform diameter configuration at $Re_D=10^3$.

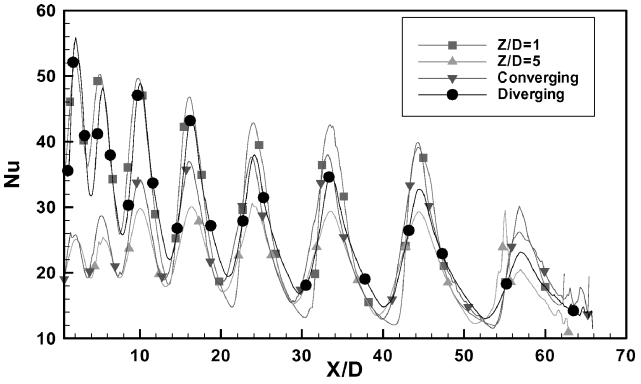

Fig. 9 Spanwise-averaged Nusselt numbers for increasing diameter configuration at $Re_D=6\times10^3$.

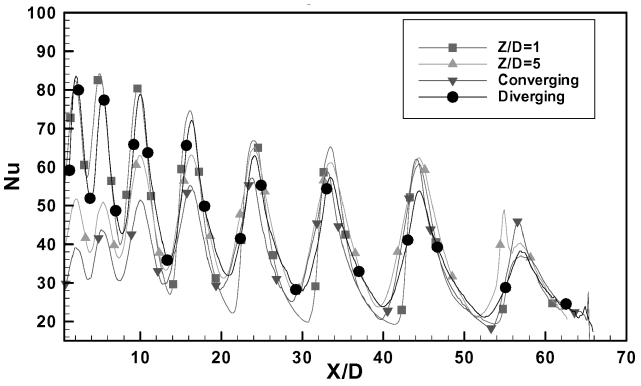

Fig. 10 Spanwise-averaged Nusselt numbers for increasing diameter configuration at $Re_D=10^3$.

Figures 9 and 10 present the spanwise-averaged heat-transfer coefficients for the increasing diameter case for each Z/D spacing and Reynolds number. The Nusselt numbers are plotted against normalized flow direction X/D. This configuration showed the best correlation to the parallel plate study of $Z/D=1$ and 5, by Gao et al.[15] Figure 9 shows the spanwise-averaged heat-transfer coefficients for $Re_D=6\times10^3$. The line for the diverging configuration lies on top of the $Z/D=1$ case for the first few holes. It falls right between $Z/D=1$ and 5 in the middle of the plate and again completely agrees with the $Z/D=5$ study for the latter jets. The same relation is seen for the converging case; except it is reversed: $Z/D=5$ on the left and $Z/D=1$ on the right. The agreement of the increasing diameter case and the constant Z/D study is more exact throughout the entire test plate than for the uniform diameter plate because there is significantly less crossflow in this configuration. These trends are also visible in Fig. 10 for airflow at $Re_D=10^3$, but like the uniform diameter case slightly more deviation from the parallel plate study occurs because at higher Reynolds number crossflow has a larger effect on the impingement results.

Comparison with Published Correlations

Kercher and Tabakoff[2] presented an impingement heat-transfer correlation based on a degradation coefficient. The impingement Nusselt number can be calculated from two functions ϕ_1 and ϕ_2 and a correction factor from the nondimensional jet-to-target pacing

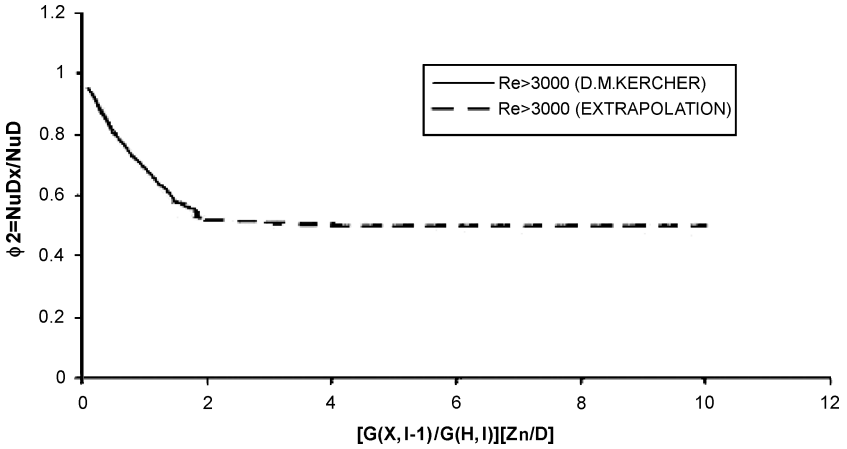

Fig. 11 Degradation of ϕ_2 coefficient as shown by Kercher and Tabakoff[2] and extrapolation.

(Z/D) as

$$Nu_D \text{ with crossflow } = \phi_1 \phi_2 Re_D^m Pr^{\frac{1}{3}} (Z/D)^{0.091}$$

where

$$\phi_1 = Nu_D Re_D^{-m} Pr^{-\frac{1}{3}}$$

for Z/D without crossflow, and

$$\phi_2 = \frac{Nu_{\text{with crossflow}}}{Nu_{\text{without crossflow}}}$$

The term ϕ_2 is called the degradation coefficient and is plotted against the term crossflow to jet flow mass flux ratio $[G(X, I-1)/G(H, I)]$, where $G(X, I-1)$ is the mass flux ratio at streamwise distance X and $(I-1)$th row and $G(H, I)$ is at the Ith row and the local jet-to-target plate spacing Zn/D. Figure 11 presents the variation of ϕ_2 vs $[G(X, I-1)/G(H, I)]|Z_n/D|$. However, the measured range for their study for the x axis value was up to 1.7. In our study, especially for variable arrays, we have x-axis values as high as 9, resulting in a need for extrapolation. If we just extend the curve in the same degradation levels as for the earlier values, we reach values for ϕ_2 that produce negative Nusselt-number values. To avoid this problem, we chose to maintain constant values of ϕ_2 for x-axis values greater than 2.0. This produced reasonable results for Nusselt numbers.

Florschuetz et al.[5] presented another correlation for jet-impingement heat transfer with crossflow effects. They arrived at a more detailed correlation given as

$$Nu = A Re_j^m \left\{1 - B[(Z/D)(G_c/G_j)]^n\right\} Pr^{\frac{1}{3}}$$

The values of A, m, B, and n depend on the pattern of the jet arrays. In our study, we treated each row as independent inline row considering that we truly do not have either staggered or inline patterns in the traditional sense. The values for the constants and exponents are obtained from the table provided in the paper. Using the preceding two correlations and the measured mass fluxes at each row, the local heat-transfer coefficients have been predicted for both uniform and variable diameter arrays. The local diameter of the jet hole and the Z/D spacing were used in the correlation to determine the local average heat-transfer coefficients for each row. Both of these studies[2,5] presented correlations that provide regional average or plate average Nusselt numbers and not local distributions as obtained in the present study. Also these predictions were calculated for parallel plate flow. Some changes in crossflow measurements could be seen in converging and diverging configurations as a result of pressure gradients in the streamwise direction.

Figures 12–15 present the regional average heat-transfer coefficient comparisons for uniform and increasing diameter configurations and the predictions from both correlations for $Z/D = 3$. Figures 12 and 13 show this comparison for the uniform diameter case at $Re_D = 6 \times 10^3$ and 10^3 with a converging, diverging,

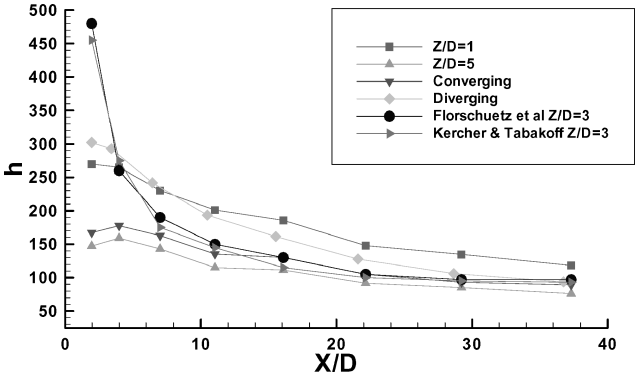

Fig. 12 Comparison of experimental data to published correlations for the uniform diameter cases at $Re_D = 6 \times 10^3$.

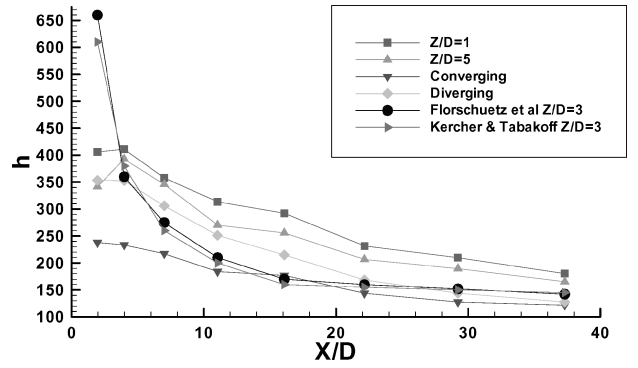

Fig. 13 Comparison of experimental data to published correlations for the uniform diameter cases at $Re_D = 10^3$.

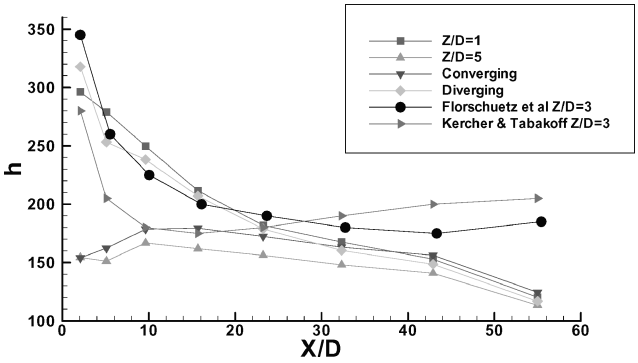

Fig. 14 Comparison of experimental data to published correlations for the increasing diameter cases at $Re_D = 6 \times 10^3$.

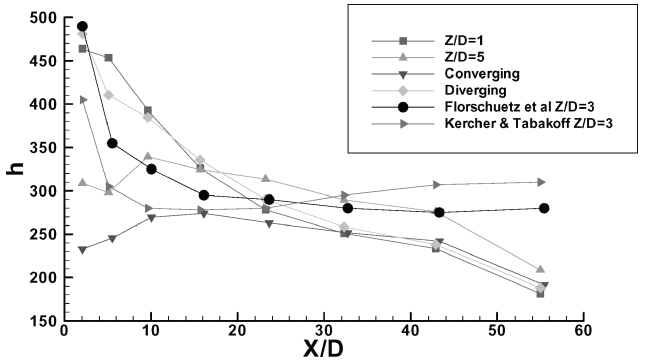

Fig. 15 Comparison of experimental data to published correlations for the increasing diameter cases at $Re_D = 6 \times 10^3$.

$Z/D = 1$, and $Z/D = 5$ impingement channel. One would expect a good prediction for $Z/D = 3$ to fall in between the converging and diverging cases at the first and last holes because at these locations on configuration it is at $Z/D = 1$ and the other at $Z/D = 5$. However, in this plot both correlations predict very high heat-transfer coefficients for the first row and show immediate degradation downstream for the rest of the rows. The heat transfer in the first row is severely overpredicted, as the correlation uses no crossflow at this point. As the correlation considers points downstream towards the exit and starts accounting for crossflow, it begins to more accurately predict the heat-transfer coefficients.

The comparison of the predicted heat-transfer coefficients and the actual data for the increasing diameter cases are shown in Figs. 14 and 15. Here regional averages of heat-transfer coefficients for converging, diverging, $Z/D = 1$, and $Z/D = 5$ are presented for $Re_D = 6 \times 10^3$ and 10^3 along with predicted results. In this configuration the overprediction and lack of crossflow consideration for both correlations were present, but not as severe. This is seen because the correlation lines and the diverging lines are quite similar; however, the correlation line predicts heat-transfer coefficients for a $Z/D = 3$, and the diverging case has a $Z/D \approx 1$ at that point. These correlations' overprediction is not as large in the increasing diameter case because the crossflow is not as severe because of the small hole diameters in the first rows. The correlations perform the best at the middle of the plate where the Z/D spacing of the converging and diverging cases is closer to three. Finally, at the last rows of the increasing diameter cases it seems that the correlations are again overpredicting the heat transfer, but when one considers the fact that the Z/D spacing at the exit of the diverging case is close to five, these predictions might make sense. As for the converging case, the spacing at the exit is actually close to one, so that it would seem that the correlation should be lower than the experimental results. The accelerating crossflow experienced by impingement jets towards the exit of the converging channel is probably responsible for this discrepancy.

Conclusions

Detailed heat-transfer distributions were measured for different impingement arrays configurations in converging and diverging channels. The heat-transfer measurements were then compared to results for parallel plate channels of different jet-to-wall spacing and predictions by correlations without pressure gradient effects. For each of the jet plate arrays, the results clearly show that the streamwise pressure gradient causes significant effects on the heat-transfer distributions. The crossflow is affected by the acceleration in the converging channels and deceleration in the diverging channels. The changes in crossflow impact the impingement strength of downstream holes that are typically subject to stronger crossflows. Comparisons of the results show that the parallel channels with even spacing throughout show similar trends where the converging channels match in dimension. When the walls are spaced $Z/D = 1$, then the converging channel will have similar dimensions at the exit. The results for $Z/D = 1$ constant channel match at the exit of the converging channel. Similarly for the diverging channels, this trend is clearly evident. Also, the results are predicted relatively well with the accepted correlations for impingement heat transfer. More detailed flow measurements and correlation analysis are required to determine the smaller variations that are caused as a result of streamwise pressure gradient effect.

Acknowledgments

The authors acknowledge the support from the project funded by Louisiana Board of Regents through the NASA-LaSPACE REA under contract from NASA/LEQSF. The program manager is John Wefel. Acknowledgments are also given to Hasan Nasir for help with the initial design and experimental setup.

References

[1]Chupp, R. E., Helms, H. E., McFadden, P. W., and Brown, T. R., "Evaluation of Internal Heat Transfer Coefficients for Impingement Cooled Turbine Blades," *Journal of Aircraft*, Vol. 6, No. 1, 1969, pp. 203–208; also AIAA Paper 68-564, 1968.

[2]Kercher, D. M., and Tabakoff, W., "Heat Transfer by a Square Array of Round Air Jets Impinging Perpendicular to a Flat Surface Including the Effect of Spent Air," *Journal of Engineering and Power*, Vol. 92, No. 1, 1970, pp. 73–82.

[3]Chance, J. L., "Experimental Investigation of Air Impingement Heat Transfer Under an Array of Round Jets," *TAPPI*, Vol. 57, No. 1, 1974, pp. 108–112.

[4]Florschuetz, L. W., Berry, R. A., and Metzger, D. E., "Periodic Streamwise Variation of Heat Transfer Coefficients for Inline and Staggered Arrays of Circular Jets with Crossflow of Spent Air," *Journal of Heat Transfer*, Vol. 102, No. 2, 1980, pp. 132–137.

[5]Florschuetz, L. W., Truman, C. R., and Metzger, D. E., "Streamwise Flow and Heat Transfer Distribution for Jet Impingement with Crossflow," *Journal of Heat Transfer*, Vol. 103, 1981, pp. 337–342.

[6]Behbahani, A. I., and Goldstein, R. J., "Local Heat Transfer to Staggered Arrays of Impinging Circular Air Jets," *Journal of Engineering and Power*, Vol. 105, No. 3, 1983, pp. 354–360.

[7]Florschuetz, L. W., Metzger, D. E., and Su, C. C., "Heat Transfer Characteristics for Jet Array Impingement with Initial Crossflow," *Journal of Heat Transfer*, Vol. 106, No. 1, 1984, pp. 34–41.

[8]Downs, S. J., and James, E. H., "Jet Impingement Heat Transfer—A Literature Survey," American Society of Mechanical Engineers, Paper 87-HT-35, Nov. 1987.

[9]Huber, A. M., and Viskanta, R., "Comparison of Convective Heat Transfer to Perimeter and Center Jet in a Confined, Impinging Array of Axisymmetric Air Jets," *International Journal of Heat and Mass Transfer,* Vol. 37, No. 18, 1994, pp. 3025–3030.

[10]Huber, A. M., and Viskanta, R., "Effect of Jet-Jet Spacing on Convective Heat Transfer to Confined, Impinging Arrays of Axisymmetric Air Jets," *International Journal of Heat and Mass Transfer,* Vol. 37, No. 18, 1994, pp. 2859–2869.

[11]Van Treuren, K. W., Wang, Z., Ireland, P. T., and Jones, T. V., "Detailed Measurements of Local Heat Transfer Coefficient and Adiabatic Wall Temperature Beneath an Array of Impingement Jets," *Journal of Turbomachinery,* Vol. 116, No. 2, 1994, pp. 369–374.

[12]Huang, Y., Ekkad, S. V., and Han, J. C., "Local Heat Transfer Coefficient Distribution Under an Array of Impinging Jets Using a Transient Liquid Crystal Technique," *Journal of Thermophysics and Heat Transfer*, Vol. 12, No. 1, 1998, pp. 73–79.

[13]Bailey, J. C., and Bunker, R. S., "Local Heat Transfer and Flow Distributions for Impinging Jet Arrays of Dense and Sparse Extent," American Society of Mechanical Engineers, Paper GT-2002-30473, June 2002.

[14]Ekkad, S. V., Gao, L., and Hebert, R. T., "Effect of Jet-to-Jet Spacing in Impingement Arrays on Heat Transfer," American Society of Mechanical Engineers, Paper IMECE2002-32108, Nov. 2002.

[15]Gao, L., Ekkad, S. V., and Bunker, R. S., "Impingement Heat Transfer, Part I: Linearly Stretched Arrays of Holes," *Journal of Thermophysics and Heat Transfer* (submitted for publication).